

Experimental Modal Analysis for a T09 AEROMAX type Aircraft's Mechanical Structure

Javier Leal-Gutierrez
Departamento de Ingeniería
Universidad Aeronáutica en Querétaro
Querétaro, México
5305@soyunaq.mx

David Romero-Gonzalez
Departamento de Ingeniería
Universidad Aeronáutica en Querétaro
Querétaro, México
5419@soyunaq.mx

Oscar A. Garcia-Perez
Departamento de Ingeniería
Universidad Aeronáutica en Querétaro
Querétaro, México
oscar.garcia@unaq.mx

Abstract—The present study investigates alternatives to incorporating energy harvesting into the aerospace field. Specifically, this energy harvesting will be focused on identifying the natural frequencies of a T09 Aeromax model aircraft's wing and proposing installation locations for piezoelectric patches. This objective was completed using experimental and numerical modal analyses and iterating based on each trial's results combined with the use of vibrations table. At the same time, a new methodology is proposed for future researchers to develop their finite element model for modal analysis for any model aircraft if the identified influencing variables are considered, and enough iterations are run. Two location proposals for patch installation are presented based on the accelerometer measurements obtained from the DynaView software, the natural frequencies obtained, and the data recollected from modal shapes and their respective deformations.

Keywords—Aircraft, energy harvesting, piezoelectric patch, modal analysis, structural dynamics.

I. INTRODUCTION

Every day technology advances towards automation, allowing the construction of tools or vehicles that make specific tasks easier or even taking human interaction out of the equation. On the other hand, there is an apparent need in the aerospace industry for unmanned aircraft, or UAVs, for military, recreational, or even commercial use. Combined with more sustainable design and manufacturing processes, any product will become more desirable [1]. Researching a technology that can turn aircraft into self-charging structures will represent an increase in mechanical efficiency, meaning the vehicle can extract mechanical energy from any of the effects that may occur in regular operation [2]. The goal would be to harvest and convert this energy into another type that may be redirected towards other systems needed in flight. A common type of impact airplanes suffer in flight is mechanical vibrations; by using piezoelectric patches, it is hypothesized that these elements will be suitable for harvesting the kinetic energy from these mechanical vibrations [3]. Given this, the

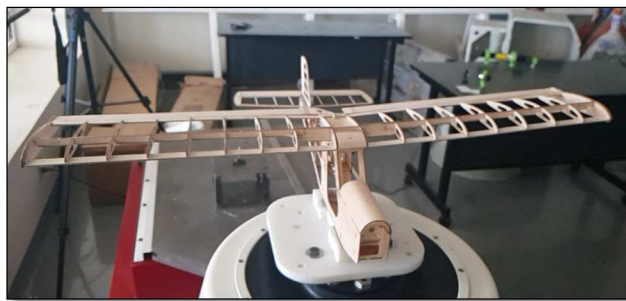


Fig. 1. Aircraft to fixture coupling

structural dynamics of an airplane must be evaluated with experimentation and modal analysis to determine how a piezoelectric patch should be installed. For this research, a T09 Aeromax trainee model aircraft will be used to determine a location for installing these patches on the wing and develop a methodology that will allow researchers to study the structural dynamics of an aircraft for future development.

Modal Analysis

A modal analysis consists of finding the natural frequencies of a system given a particular combination of mass, stiffness, and damping elements that the system has against mechanical vibrations. When the vibration input has a frequency equal to any of the system's natural frequencies, a consistent rise of mechanical strain is exerted on specific elements that may fatigue the structure or even break it apart [4]. This effect is known as resonance, and the mechanical strain increase follows an exponential behavior. The displacements and deformations that occur in resonance are particular for each natural frequency, also known as modal shapes [5], [6].

II. RESULTS

For modeling the aircraft, it is recommended for the user to scan and scale each component on a CAD model for higher precision before starting the Experimental Modal Analysis (EMA).

A. Experimental Modal Analysis

It is fundamentally necessary that before starting any procedure, a scope is developed according to the capabilities of the study. This scope means having previous knowledge of how many tools and instruments can be provided and the parameters that the available machinery allows for the experiment. Secondly, it is also necessary to always have a mindset toward possible readjustments in modal analysis, given that too many variables may affect the numerical model, making the process very iterative.

Initially, the aircraft model was constructed in three different stages:

- Wing
- Fuselage
- Empennage

The main reason behind the separation in various stages is to allow for an independent wing analysis alongside an analysis of the whole aircraft assembly. For the wing, it was built in such a manner that no fixture was needed to mount it on the vibration test table. Unfortunately, this was not the case for the complete model of the aircraft. In this case, a fixture was designed so that its dynamics would not interfere with the dynamics of the wing when mounted on the vibration test table as shown in Fig. 1. The design was 3-D printed with ABS plastic, and a complete modal analysis of the fixture was conducted to validate its worthiness for the experimental process.



Fig. 2. Mounting Accelerometer



Fig. 3. Data acquisition system.

For the first iteration, it is fundamental to prove that the accelerometer's measurements can be trustworthy and that this component will not be exposed to an experimental environment that might reach its design capability limits. For this reason, a first test was conducted without any wing or aircraft sensor. The plane was subjected to vertical oscillations using a frequency sweep from 0 to 100 Hz to visualize and approximate the actual natural frequency values. After analyzing that no mode shapes have enough amplitude to interfere with the sensor, a PCB accelerometer was mounted on the left-wing tip connected to an NI USB-4431 for vibration data acquisition as shown in Fig. 2 and Fig. 3, respectively. In combination with the DynaView software, the same frequency sweep was manually conducted a second time to provide more accurate frequency measures. Where the FFT graph presented any peaks, this would translate into the natural frequencies of the model, and these values were compared against the visualized values obtained on the first trial. For means of the accelerometer measurements validation, these values would also be compared against the numerical modal analysis on each of its iterations. Given the results obtained from these first tests and their comparison versus the iterations conducted for the numerical modal analysis, the experiment was readjusted to add the other two axes (X and Y) as shown in Fig. 4 and Fig. 5. The main reason for adding more axes orientations for vibration inputs is because some modal shapes were concealed in the first exclusively vertical vibrations and only appeared for a specific orientation. This would also lead to analyzing the model aircraft in combined axes vibrations to see if any of the modal shapes might even combine, showing more shapes that only the numerical model predicted (validating if the model is now truthful). Another change was that the accelerometer was installed in the left vertical stabilizer to validate certain natural frequencies, given that specific modal shapes were only present on the empennage stage.

B. Numerical Modal Analysis

First handedly, it is essential to mention that the Numerical Modal Analysis (NMA) must be truthful to the EMA results, given that the essence of having an accurate numerical model is to simulate the real events that happen in the actual model. For this experiment, a simple FEA was conducted using a Solidworks Student License, and in this case, only three iterations were needed to converge into trustful results.

Mainly, three variables were extracted as those with more predominance over the NMA results:

- Boundary Conditions (BC)
- Material Properties
- Mesh Attributes

Starting with the BCs, it is essential to acknowledge the effects of the vibration table and the fixture on the wing or the model, respectively. Given that screws were used to clamp the wing onto the table, a fixed condition was applied to the planar surface that would make contact in the EMA process. Analogically, the planar surface that would make contact between the fuselage's floor and the fixture was also fixed.

In the case of setting up material properties for each study, aircraft model suppliers prefer the use of Balsa wood as the primary structural material. Given this information, it is also critical to acknowledge that Balsa wood has fibers that allow the material to behave distinctively depending on the orientation of a stress input as shown in Fig. 6. This property would mean that Balsa wood is orthotropic and not isotropic. However, it was unknown how much impact this variable would have on the NMA, so standard isotropic material properties for Balsa wood were applied for the first study, resulting in significant deviations from the EMA's first trial. Given these deviations, a second reference for Balsa wood properties was applied, where values for each axis E relative to the fibers' orientation were provided for it to behave as an orthotropic material. This change would substantially close the gap between the EMA's results but not close enough for validating a precise NMA. For the final iteration, a third reference was researched where the E values were barely different while reporting the same values for μ of each plane.

Finally, the main parameter guiding the decisions for the mesh attributes is the available computer power versus the available time. In this case, the computer power was limited to the available nodes that a modal analysis can carry in a Solidworks Student License. However, in most cases, this does not apply since the available resources dictate a computer's limitations for processing data, which might be RAM and GPU, among others. Without sufficient power, the simulation might take significantly more time to converge results or, in some cases, even crash and never be able to process the data. This case is where time becomes a valuable factor since deadlines might also dictate the experiment's lifespan, and if these are not met, it will end up in a waste of resources. The mesh is how a CAD model is separated into fine elements; the computer uses each element to calculate the properties shared with their surrounding elements. A finer mesh has many more minor elements that constitute the model, meaning that the results will be more accurate but will also make the computer consider more elements for calculation—consequently, taking more time and power to solve the simulation. However, the other end is a coarse mesh, where elements are significant in size and less in numbers, meaning that the computing power and time will not be a problem. However, perhaps curved or more complex geometries will not represent the original model meaning the obtained results might not be truthful. This stage is where a balancing act is applied, where finding a sufficiently fine mesh that will allow for results that are just as precise as needed and a not-so-fine mesh so that it will not consume more power and take more time for unnecessary precision.

In this experiment, the empennage elements were smaller and thinner, and many problems arose in the construction and assembly process. For this main reason, it was decided to implement a relatively finer mesh at this stage than on the rest of the model.

The results will be shown in order of appearance to indicate the methodology iteration and trial steps. Even though it was possible to obtain conclusive results in three iterations, it is highly recommended for any researcher following this methodology to conduct as many iterations as needed so that he/she can also converge into conclusive results. Table I shows the description first twelve

modal shapes computed using NMA, which will be useful to validate the numerical model.

A. First trial - EMA

Table II shows the first nine natural frequencies found for the first experimental trial of the complete model aircraft. The data shows the deviation between the visually obtained results and the accelerometer measurements, as well as the results for the first NMA iteration. It is essential to mention that the highest deviation is weighted at 8.5%, which is not desirable. For precise analysis, it would be necessary to make the NMA as accurate as possible to allow for accelerometer measurement validation. It is also important to mention that many modal shapes could not be described with clarity, which, combined with the analysis, directed the experiment to be readjusted to add the other two axes.

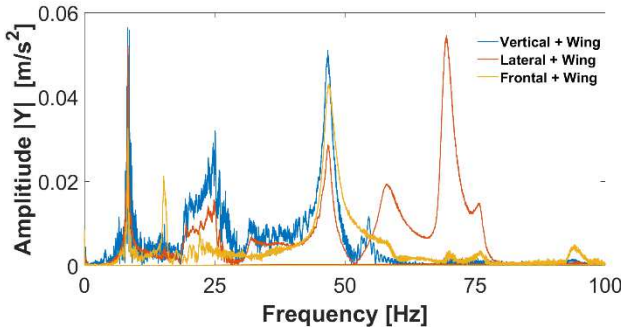


Fig. 4. Aircraft Natural Frequencies – 2 locations accelerometer mounting (Main Wing)

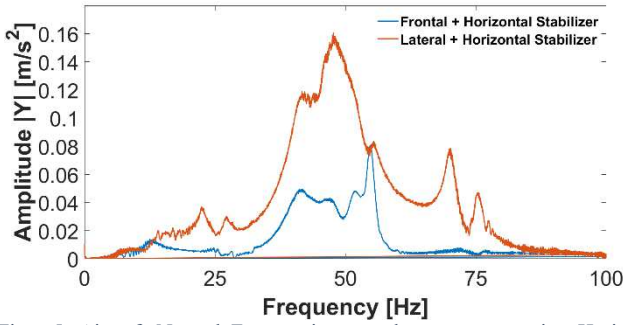


Fig. 5. Aircraft Natural Frequencies – accelerometer mounting Horizontal Stabilizer

B. Second Trial - NMA Iterations

Table III shows how results converged to the first data set obtained from the 1st EMA trial. Given that the highest deviation from the first data set stood at 4.42%, it was decided to stop iterating the NMA. A significantly finer mesh

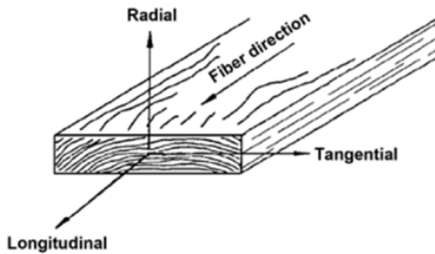


Fig. 6. Orthotropic Properties of Wood [7].

would have been necessary for further precision, and it was uncertain how much additional computing power and time this process might have consumed.

On the other hand, despite all the efforts, the exclusive analysis conducted for the wing could not converge in any of the iterations to any desired results. This effect will be discussed further on in this study report.

TABLE I. Aircraft Modal Shapes Description.

Modal Shape	Description
1	Location: Antinode at wing’s trailing edge on the main wing tip. Displacement: Alternating movement between semi-spans; flexion with a slight torsion relative to the Z axis.
2	Location: Antinode at wing’s trailing edge on the main wing tip. Displacement: Simultaneous movement between semi-spans; flexion with slight torsion relative to the Z axis.
3	Location: Antinode at wing’s trailing edge on the main wing tip. Displacement: Alternating movement between semi-spans; torsion relative to the XZ plane.
4	Location: Antinode at wing’s leading edge on the main wing tip. Displacement: Right semi-span - flexion with a moderate torsion relative to the Z axis. Left semi-span - flexion relative to the X axis.
5	Location: Antinode at wing’s trailing edge on the main wing tip. Displacement: Simultaneous movement between semi-spans; torsion relative to the XZ plane.
6	Location: Antinode at horizontal stabilizer’s wing tip. Displacement: Horizontal Stabilizer - Alternating movement between semi-spans; flexion relative to the Z axis. Vertical Stabilizer - Small oscillating flexion relative to the Y axis.
7	Location: Antinode at horizontal & vertical stabilizer’s wing tips. Displacement: Horizontal Stabilizer - Alternating movement between semi-spans; flexion relative to the Z axis. Vertical Stabilizer - Moderate oscillating flexion relative to the Y axis.
8	Location: Antinode at main wing & horizontal stabilizer’s wing tips. Displacement: Main Wing (Most predominant) - Simultaneous movement between semi-spans; flexion relative to the X axis. Horizontal Stabilizer: Simultaneous movement between semi-spans; flexion relative to the Z axis.
9	Similar to previous modal shape with the distinction of having the most predominant displacement located at the horizontal stabilizer.
10	Location: Antinode at horizontal & vertical stabilizer’s wing tips. Displacement: Horizontal Stabilizer: Alternating movement between semi-spans; flexion relative to the Z axis. Vertical Stabilizer (Most Predominant): Moderate oscillating flexion relative to the Y axis.
11	Location: 2 Antinodes; first one located at one-third distance of the semi-span’s trailing edge. Second one located at the wing’s tip trailing edge. Displacement: Alternating movement between semi-spans; flexion relative to the Z axis. Main torsion at the semi-spans created by the antinode displacements. Highest displacement at right semi-span section.
12	Similar displacement as the previous modal shape with the distinctions that the movement is simultaneous instead of alternating between semi-spans and that the most main displacement is located at the left semi-span.

C. Third Trial - EMA iterations

Given the necessary readjustments, Fig. 3 shows the accelerometer readings from Dynaview for the different vibration orientations for the wing and vertical

stabilizer, respectively. This information was extracted into Table IV to read which axis predominated each modal shape more clearly and compare the FFT peaks against the NMA results. For the trials with the accelerometer mounted on the wing, the highest deviation measured at 6.2% and the lowest at 0%, validating the NMA for future trials. However, for the trials with the accelerometer mounted on the vertical stabilizer, massive deviations occurred, topping up to 46%. This result could infer that the NMA is not precise enough. Nevertheless, considering that the scope was to validate the wing's dynamics throughout the wing and the complete model, the NMA's objective was completed successfully.

TABLE II. First trial – EMA

Mode Shape	Frequencies [Hz]		
	ω_n accel (Hz)	ω_n sight (Hz)	ω_n NMA (Hz)
N/A	11.3	12.0	NA
2	17.7	17.0	15.8 Hz
NA	24.1	22.0	NA
5	32.	32.5	29.8 Hz
NA	35.0	35.0	NA
8	58.6	53.2	46.1 Hz
9	68.9	67.5	47.7 Hz
11	76.1	75.7	73.3 Hz
12	89.9	87.3	86.2 Hz

TABLE III. Second trial - CMA Iterations

Mode Shape	Frequencies (Hz)		
	1st Iteration (Hz)	2nd Iteration (Hz)	3rd Iteration (Hz)
1	21.2	11.5	12.3
2	25.9	15.8	16.6
3	43.7	25.0	25.9
4	46.9	25.8	27.7
5	47.7	29.8	30.6
6	51.5	34.8	37.9
7	63.4	40.0	43.8
8	69.6	46.1	49.8
9	111.3	47.7	52.5
10	117.3	57.1	62.2
11	144.2	73.3	77.8
12	156.1	86.0	89.8

TABLE IV. Third Trial - EMA

Mode Shape	Frequencies (Hz)			
	ω_n accel (Hz)	ω_n sight (Hz)	ω_n NMA (Hz)	Most contributive axis
1	12.2	13.0	12.3	Y
2	17.7	17.0	16.6	Z
3	24.9	23.9	25.9	Y
5	32.6	32.5	30.6	Z
8	46.3	53.2	49.8	X
10	60.0	60.7	62.2	Y
9	68.9	67.5	52.5	Z
7	70.2	71.0	37.9	Y
11	76.1	75.7	77.8	Z
12	89.8	87.3	89.8	Z

III. ANALYSIS

In many cases for the EMA and NMA results, some natural frequencies and their modal shapes had a minimum to almost no deviation between them. The only difference in these cases was the side of the wing in which the main deformations occurred. This effect was probably due to an imbalance while constructing the model; such an effect must be avoided at all costs. However, given that this imbalance was also translated into the numerical model, the NMA could accurately simulate the actual model constructed in real life. This accuracy was possible given the sufficient data recollection from the EMA iterations to make a valuable comparison.

As mentioned, the EMA and NMA exclusively on the wing did not bring up conclusive results, presenting unpredictable behaviors on the modal shapes and many discrepancies between the NMA and experimental models. This effect was probably due to not simulating the BCs correctly from the wing with the vibration table. Moreover, it is recommended for any researcher following this methodology to use a whole aircraft model with the wing, fuselage, and empennage to reduce any loss of information.

The accelerometer, in combination with the DynaView software, allowed for hidden modal shapes at plane sight. The sensor's measurements were validated by a direct comparison between each trial of the NMA against the visually obtained frequencies.

IV. CONCLUSIONS

Two different installation locations are proposed according to the graphs presented above in Fig. 4 and Fig. 5. Considering that the highest peaks represent higher accelerations, this would translate into more kinetic energy that might be available for energy harvesting.

The first location is proposed according to the modal shape that was more present among all the natural frequencies. Given that most natural frequencies have a vertical deformation, the proposed zone involves installing a piezoelectric patch on the wing section on the wing's "skin" connected to the fuselage. Another main advantage of this option is that the first two natural frequencies found overall have the same modal shape, meaning that the possibility of the aircraft vibrating according to these is high.

The second proposal is according to the natural frequency with the higher-most peak on the graph (excluding the vertical stabilizer). However, in this case, the modal shape oscillated transversely, alternating between front and back instead of up and down as in the previous location. For this modal shape, a piezoelectric patch should be installed in one of the wings supporting beams for it to receive

any kinetic energy. Given that both proposals allow for a flexible patch installation, a bending type of patch is recommended for the study. However, given that patch sizes and dimensions depend on each provider, this selection process will be held until future research.

It must be noted that these graphs present highly damped modes, and it might lead to the conclusion that it is due to a non-linearity behavior. However, this phenomenon can be explained by the close proximity between natural frequencies; in the **b) graph** specifically it can be determined that the mixed orientations on the modal shapes where the causing elements since when a natural frequency is ending, another one is barely starting. Furthermore, noting that for a modal analysis to take place an exclusive structural damping factor must be considered.

Both options are limited to a proposal standpoint since this methodology does not evaluate the effects of aeroelasticity. This study should be conducted in the future, given that the deformations that may occur in a static analysis might not be the same as the ones presented in-flight. This study, along with three other previously discussed complications, implies different areas for future research: An exclusive study on the vertical stabilizer is recommended to obtain enough precision in this area. Adding combinations of vibration orientation inputs to analyze closely any mixed modal shapes.

Conducting an aeroelastic study focused on the three main stages of flight (take-off, cruise, and landing).

Upgrade the aircraft model quality from its origin to avoid any imbalance. This upgrade could come from changing the provider, maintaining a more controlled environment in the building phase, and closely examining the numerical model component versus component with the experimental model.

The methodology presented may be reproduced in other aircraft models if and only if the parameters presented are followed and conducting enough iterations to converge into reliable results. For this particular case, the NMA T09 Aeromax model is also reliable if it is going to be used to predict the actual T09 Aeromax experimental model.

Regarding the installation of a piezoelectric patch, the structure's natural damping behavior will probably be affected, mainly due to the mechanical energy being converted into electrical energy acting as an indirect damping element. Moreover, only structural damping was considered, thus by including all the additional damping factors the vibrations produced on the wing will probably stay in a certain amplitude range. In terms of the natural frequency,

these frequencies might probably shift; however, only the modal shapes determine the patch's position, meaning this frequency shift is not relevant.

The possibility of energy harvesting on wing vibrations is a possibility that requires future research; however, it does exist. It is only a matter of the researcher inquiring enough about the possible applications that this converted energy might present.

ACKNOWLEDGMENTS

The authors would like to acknowledge and give their warmest thanks to the project supervisor Dr. Garcia-Perez as well as the Universidad Aeronáutica en Querétaro (UNAQ) for the resources provided to make this work possible. The authors would also like to express their gratitude towards the support staff, especially Dr. Rojas-Ramirez that shared his knowledge for using the instruments provided.

REFERENCES

- [1] B. Gagnon, R. Leduc, L. Savard, "From a conventional to a sustainable engineering design process: different shades of sustainability". *Journal of Engineering Design*, 23 (1), pp. 49-74.
- [2] A. Erturk and D. J. Inman, *Piezoelectric Energy Harvesting*, West Sussex: Wiley, 2011.
- [3] F. Bachmann, A. Bergamini y P. Ermanni, "Optimum piezoelectric patch positioning: a strain energy-based finite element approach", *Journal of intelligent material systems and structures*, 2012, vol.23, no. 14, pp. 1575-1591.
- [4] J. Schijve, *Fatigue of Structures and Materials*, Delft: Springer, 2009.
- [5] S. Rao, *Mechanical Vibrations*, Miami: Pearson, 2017.
- [6] M. Paz & Y. Hoon Kim, *Structural Dynamics*, Cham: Springer, 2019.
- [7] D. W. Green, J. E. Winandy, D. Kretschmann, "Mechanical Properties of Wood", *Wood handbook: wood as an engineering material*. Madison, WI: USDA Forest Service, Forest Products Laboratory, 1999, pp. 45-113.